Research Square

Preprints are preliminary reports that have not undergone peer review.
They should not be considered conclusive, used to inform clinical practice,
or referenced by the media as validated information.

Turbine driven versus compressed gas ventilators for noninvasive ventilation in infants with acute respiratory failure: a randomized crossover trial

Giovanna Chidini

giovanna.chidini@policlinico.mi.it

Fondazione IRCCS Ca' Granda Ospedale Maggiore Policlinico

Domenico Luca Grieco

Università Cattolica del Sacro CuoreDepartment of

Thomas Langer

Azienda Socio Sanitaria Territoriale Grande Ospedale Metropolitano Niguarda

Cristina Villa

Fondazione IRCCS Ca' Granda Ospedale Maggiore Policlinico

Stefano Scalia Catenacci

Fondazione IRCCS Ca' Granda Ospedale Maggiore Policlinico

Tiziana Marchesi

Fondazione IRCCS Ca' Granda Ospedale Maggiore Policlinico

Maria Francesca Patria

Fondazione IRCCS Ca' Granda Ospedale Maggiore Policlinico

Giacomo Grasselli

Fondazione IRCCS Ca' Granda Ospedale Maggiore Policlinico

Edoardo Calderini

Fondazione IRCCS Ca' Granda Ospedale Maggiore Policlinico

Cesare Gregoretti

Unicamillus International Medical School

Research Article

Keywords: Noninvasive ventilation, patient–ventilator asynchrony, infants, turbine-driven ventilator, esophageal pressure, acute respiratory failure

Posted Date: August 7th, 2026

DOI: https://doi.org/10.21203/rs.3.rs-10527671/v1

License: This work is licensed under a Creative Commons Attribution 4.0 International License. Read Full License

Additional Declarations: No competing interests reported.

Abstract

Background. The performance of intentional-leak single-limb and dual-limb turbine-driven ventilators versus dual-limb compressed-gas pediatric ventilators has not been systematically evaluated during noninvasive ventilation (NIV) in pediatric respiratory failure. We therefore conducted a randomized crossover physiological study to compare patient-ventilator interaction across these three ventilator configurations in infants with acute respiratory failure.

Methods. In this single-center, randomized, crossover physiological study each infant underwent three 30-minute NIV phases, in randomized order, with constant ventilator settings: intentional-leak single-limb turbine ventilator (SLC-Turbine), dual-limb turbine ventilator (DLC-Turbine) with active expiratory valve, and dual-limb compressed-gas pediatric ventilator (DLC-PICU). Esophageal pressure was used to assess patient-ventilator interaction (Asynchrony Index [AI] and individual asynchrony events). The primary end point was the difference in AI between DLC-PICU and SLC-Turbine, and the secondary end point the difference in AI between DLC-PICU and DLC-Turbine. Breathing pattern and respiratory effort were explored by comparing the three ventilator configurations with unassisted spontaneous breathing.

Results. Twenty infants entered the stabilization phase, 13 were randomized, and 12 completed the crossover protocol and were analyzed (age 10 [7–21] months; SpO_2/FiO_2 185 [160–220]). AI differed significantly across configurations (7.5% [0–13.7], 16.8% [7.6–25], and 34.2% [17.4–67] with SLC-Turbine, DLC-Turbine, and DLC-PICU, respectively; p=0.0001). AI was higher with DLC-PICU than with SLC-Turbine (primary end point: HL +33.0, 95% CI +23.5 to +41.6; p=0.0001) and than with DLC-Turbine (secondary end point: HL +24.2, 95% CI +15.4 to +32.7; p=0.0001). Ineffective efforts did not differ across configurations. Auto-triggering was significantly higher with DLC-PICU than with SLC-Turbine (4 [0-12.5] vs 0 [0-0] events/min; p=0.0001), whereas it did not differ between DLC-PICU and DLC-Turbine. Late cycling was significantly more frequent with DLC-PICU than with SLC-Turbine (0 [0-10] vs 0 [0-0] events/min; p=0.002), whereas no significant difference was observed between DLC-PICU and DLC-Turbine.

Despite marked differences in patient–ventilator synchrony, respiratory muscle effort was similar across the three configurations, with no difference between SLC-Turbine and DLC-PICU in esophageal pressure swing (7.6 vs 7 cmH_2O; p=0.540) or esophageal pressure–time product (180 vs 135 $cmH_2O \cdot s \cdot min^{-1}$; p=0.898).

Conclusions. Compared with the compressed-gas pediatric ICU ventilator, both turbine configurations improved patient-ventilator interaction, with the single-limb configuration providing the greatest reduction in asynchrony.

Clinical trial registration. ClinicalTrials.gov, NCT04017780. Enrolment was originally planned to start in 2019 but was postponed because of the COVID-19 pandemic; patients were subsequently enrolled between January 2022 and December 2025.

Background

Noninvasive ventilation (NIV) delivered as flow-triggered pressure support is increasingly used in infants with acute respiratory failure across pediatric intensive care units (PICUs), hospital wards, and emergency departments [1–3]. Its success depends not only on ventilatory assistance but also on patient-ventilator interaction: improved synchrony is associated with greater comfort and reduced work of breathing, whereas asynchrony may impair NIV effectiveness and prolong PICU stay [4–7]. Synchrony is challenged by unintentional leaks that interfere with triggering and cycling, and by differences in leak-compensation algorithms and trigger sensitivity [8–11].

NIV is delivered using different ventilator technologies and circuit configurations. PICU ventilators typically use dual-limb circuits (DLCs) with active expiratory valves, whereas turbine-driven ventilators use single-limb circuits (SLCs) with intentional leaks through whisper valves or vented masks [12–15]. Despite their widespread use, the physiological impact of these configurations on patient-ventilator interaction has not been directly evaluated in infants. We therefore conducted a randomized crossover physiological study in infants with moderate acute respiratory failure, comparing a turbine-driven ventilator with single-limb intentional-leak circuit (SLC-Turbine), the same turbine-driven ventilator with dual-limb circuit and active expiratory valve (DLC-Turbine), and a pediatric ICU ventilator with dual-limb circuit (DLC-PICU), to determine how ventilator type and circuit configuration influence patient–ventilator synchrony, breathing pattern, and respiratory effort.

Methods

Study Design and Ethics.

This is a single-center, physiologic, randomized, crossover trial conducted at the PICU of Fondazione IRCCS Ca’ Granda Ospedale Maggiore Policlinico, Milan, Italy (January 2022 to December 2025). The protocol was approved by the Comitato Etico Milano Area 2 (approval 600_2019bis, 18 June 2019), and written informed consent was obtained from parents or legal guardians. The study was prospectively registered at ClinicalTrials.gov (NCT04017780). Enrolment was originally planned to start in 2019 but was postponed because of the COVID-19 pandemic; patients were subsequently enrolled between January 2022 and December 2025. All procedures complied with the Declaration of Helsinki and results are reported according to CONSORT guidelines [16].

Endpoints.

Primary endpoint was the difference in Asynchrony Index (AI%) between NIV delivered with a dual-limb compressed-gas ICU ventilator (DLC-PICU, Babylog VN500, Dräger) and NIV delivered with a single-limb intentional-leak turbine-driven ventilator (SLC-Turbine, Astral 150, ResMed).

The secondary endpoint was the difference in AI between DLC-PICU and DLC-Turbine, allowing comparison of ventilator platforms while maintaining a dual-limb circuit configuration. The comparison between DLC-Turbine and SLC-Turbine explored the effect of circuit configuration while keeping the ventilator platform constant.

Patient-ventilator asynchrony was evaluated in all three study conditions, as prespecified in the registered protocol. The comparison between the two turbine configurations (DLC-Turbine vs SLC-Turbine) was not a formal end point and is reported as exploratory.

Breathing pattern, ventilatory mechanics and respiratory effort were analyzed as exploratory end points. The three ventilator configurations were compared with unassisted spontaneous breathing (SB), allowing comparison against the baseline respiratory pattern of each patient.

Randomization, concealment and blinding

The three-study-condition order was randomized with a computer-generated sequence (www.randomizer.org). Allocation was concealed until enrolment; the crossover design, in which each patient underwent all three study conditions, minimized selection bias.

Patient Population

Consecutive children aged 1–24 months admitted with moderate acute respiratory failure were screened for eligibility. Severity was defined by the ratio between peripheral oxygen saturation and inspiratory oxygen fraction (SpO_2/FiO_2 ratio) < 264 plus ≥ 2 of the following: tachypnea > 2 standard deviations above age norms, use of accessory muscles, or paradoxical abdominal motion [17]

Inclusion criteria: age > 30 days and < 24 months; SpO_2/FiO_2<264 while receiving supplemental oxygen; respiratory rate >2SD above the age-related norm and/or signs of inspiratory effort. Exclusion criteria: hemodynamic instability requiring fluids or inotropes; impending intubation or severe respiratory failure (PaO_2<60 mm Hg despite FiO_2≥0.6, $PaCO_2$>55 mm Hg, arterial pH < 7.25, or recurrent apneas); contraindications to esophageal catheter placement (facial trauma, varices, congenital or acquired malformations, or recent upper gastrointestinal surgery < 6 months); intracranial hypertension; palliative care for end-stage oncologic disease; and neuromuscular, mitochondrial, metabolic, or chromosomal disorders with hypotonia [18].

Study Protocol

After an initial one-hour stabilization period on NIV with a conventional pediatric ICU ventilator, each patient underwent three consecutive 30-minute NIV trials in randomized order:

1. 1. DLC-PICU: dual-limb compressed-gas pediatric ICU ventilator (Babylog VN500, Dräger, Germany).
2. 2. SLC-Turbine: turbine-driven ventilator (Astral 150, ResMed, Australia) with a single-limb circuit and intentional leak (Whisper valve).
3. 3. DLC-Turbine: the same turbine-driven ventilator configured with a dual-limb circuit and an active expiratory valve.

These three conditions were designed to disentangle ventilator technology from circuit configuration: DLC-Turbine isolated circuit type while keeping the ventilator platform constant. Breathing pattern and respiratory effort were explored by comparing the three ventilator configurations with unassisted spontaneous breathing.

During stabilization, NIV was delivered as first-line respiratory support with a conventional double limb PICU ventilator according to clinical judgment; children meeting predefined NIV failure criteria were intubated and excluded (see Safety Termination Criteria)[19]. Patients who remained clinically stable were randomized to the three conditions in a crossover design, with phases separated by a 20-minute washout period; washout recordings were excluded from all analyses.

Ventilator settings were determined before enrollment according to clinical practice and remained unchanged throughout the study. FiO_2 was adjusted to maintain SpO_2 ≥94%. Pressure support was titrated to reduce respiratory rate and chest wall retractions. PEEP was set between 4 and 8 cmH_2O (2-cmH_2O increments) while keeping FiO_2≤0.6. Rise time was set to the fastest value avoiding pressure overshoot and kept constant across all conditions.

Trigger sensitivity was individually optimized for each ventilator, selecting the highest sensitivity that avoided auto-triggering. The expiratory trigger threshold was set to the lowest value avoiding delayed cycling or inspiratory prolongation beyond neural inspiration. Minimum and maximum inspiratory times were fixed at 0.2 and 1.5 seconds to prevent time-cycled breaths while preserving flow cycling [11–20].

A pediatric full-face mask (Performax XS, Philips Respironics, The Netherlands) was used throughout to minimize unintentional leaks and ensure consistency across conditions [20–21]. Patients were studied semi-recumbent (30–45°) and received continuous dexmedetomidine (0.5–1.0 µg/kg/h), titrated to maintain a COMFORT score of 17–26; sedation was started before enrollment and kept unchanged throughout, with no additional sedatives or opioids [22–23].

NIV was discontinued if predefined safety criteria were met: hypoxemia (SpO_2<90% despite FiO_2>0.6), hypercapnia ($PaCO_2$ increase > 10% from baseline), or severe intolerance (COMFORT score > 26 despite sedation). Continuous monitoring included ECG, pulse oximetry, non-invasive blood pressure, and respiratory rate, with a senior consultant immediately available in case of adverse events.

Measurements and Definitions

Asynchrony

Asynchronies were expressed as the Asynchrony Index (AI) [7]. AI was calculated as:

AI (%) = [Number of asynchronous events / (Number of ventilator cycles + Number of ineffective efforts)] × 100

Asynchronies (PVAs) were classified as follows: ineffective effort, defined as an inspiratory effort identified on esophageal pressure (Pes) tracing that failed to trigger a ventilator-assisted breath; auto-triggering, defined as delivery of a ventilator-assisted breath in the absence of a corresponding inspiratory effort on Pes; double triggering, defined as two consecutive ventilator-assisted breaths separated by an abnormally short expiratory time and usually initiated by a single patient effort; premature cycling, defined as termination of ventilator support before completion of the patient's inspiratory effort, indicated by

persistence of negative Pes deflection after ventilator cycling; and late cycling, defined as persistence of ventilator insufflation beyond the end of the patient's inspiratory effort [7].

Physiological variables and polygraph-derived measurements

Respiratory flow was measured with a heated pneumotachograph (Fleisch No. 2; Fleisch, Lausanne, Switzerland), and airway pressure proximally between circuit and patient interface. Esophageal pressure (Pes) was measured with a radio-opaque 6-Fr balloon catheter (CareFusion, San Diego, CA, USA), inserted nasally to 15–20 cm and inflated with 0.3–0.5 mL of air [24]. After confirming a positive inspiratory pressure deflection, the catheter was gradually withdrawn until positioned in the lower esophagus, confirmed by negative inspiratory deflections and cardiac artifacts on the tracing [25]. Signals were acquired continuously at 100Hz with dedicated software (Kleistek ICU, Bari, Italy) [25, 26]. Start of inspiration was defined at Pes initial decay, and end of inspiration at 25% recovery of the Pes deflection from its nadir toward baseline [27]. Effort-per-breath was quantified as the esophageal pressure swing (ΔPes), the difference between Pes at onset of inspiratory deflection and its nadir. Effort-per-minute was quantified as esophageal pressure–time product, the area under the Pes signal below its end-expiratory value during neural inspiration, summed over one minute ($cmH_2O \cdot s \cdot min^{-1}$). Chest wall recoil pressure was not measured and was assumed constant within each patient. Signal segments with cough, agitation, suctioning, or motion artifacts were excluded. All signals were calibrated before each trial, time-synchronized, and stored for offline analysis (Additional file 1: Measurements and Definitions).

Circuit configuration

SLC-Turbine. In the single-limb configuration, an intentional leak was incorporated through a Whisper Swivel valve (Philips Respironics, Pittsburgh, PA, USA) to permit CO_2 washout. The valve consists of a fixed-resistance leak port with a calibrated pressure–flow relationship, with leak flow increasing as airway pressure rises.

DLC-Turbine. The same turbine-driven ventilator was configured with a dual-limb circuit and an active expiratory valve. No intentional leak was incorporated into the circuit.

DLC-PICU. The compressed-gas pediatric ICU ventilator was used with a dual-limb circuit and an active expiratory valve. No intentional leak was incorporated into the circuit.Active humidification was provided during all trials using an MR850 humidifier (Fisher & Paykel Healthcare) (Fig. 1: Circuit Configuration).

Data Analysis

Signals were recorded during each phase and analyzed offline by a senior investigator blinded to ventilator type, circuit configuration, and phase allocation, using anonymized tracings without access to condition labels. Analyses included identification and classification of PVAs, calculation of the AI, and computation of secondary physiologic variables; segments with artifacts, coughing, or suctioning were excluded.

Statistical analysis

Sample size was estimated for the primary endpoint (Asynchrony Index comparison between SLC-Turbine and DLC-PICU) using MedCalc Statistical Software (version 20.0; MedCalc Software Ltd, Ostend, Belgium). Based on a previously reported Asynchrony Index (AI) of 59 ± 13% and assuming a clinically relevant 20% relative reduction, 12 patients were required to achieve 80% power with a two-sided α of 0.05 for this paired comparison. Data distribution was assessed using the Shapiro-Wilk test. As data were not normally distributed, results are presented as median [interquartile range]. Overall differences among the three ventilator configurations were assessed using the Friedman test for repeated measures. When the overall test was significant, predefined pairwise comparisons were performed using the Wilcoxon signed-rank test. Effect sizes are reported as Hodges-Lehmann median differences with 95% confidence intervals (95% CI). No formal sample size calculation was performed for secondary or exploratory endpoints; therefore, these analyses should be considered supportive and hypothesis-generating. All tests were two-sided, and statistical significance was defined as $p < 0.05$.

Results

The study flowchart is shown in Fig. 2. Of the thirteen randomized patients, one was withdrawn before completing all three phases; the remaining twelve completed the protocol and were analyzed. Baseline characteristics are summarized in Table 1.

Table 1
Baseline characteristics of the study population.

Variable	Median [IQR]
Age, months	10 [7–21]
Weight, kg	9.5 [7.9–11.6]
PIM2 score	3.5 [3.0–4.3]
pSOFA score	3 [3–3]
COMFORT score	16 [16–18.8]
Length of stay in PICU, days	6 [4–6.5]
Hospital length of stay, days	9 [8–11]
Survival, n/N	12/12
FiO_2	0.50 [0.43–0.50]
SpO_2/FiO_2 ratio	185 [160–220]
$PvCO_2$, mmHg	44 [39.5–49.5]
pH, venous	7.39 [7.37–7.44]
Base excess, mmol/L	3 [– 0.1 to 6.8]
Bicarbonate (HCO_3^-), mmol/L	26 [21.8–30.3]
Respiratory rate, breaths/min	52.5 [45–60]
Lactate, mmol/L	1.0 [0.9–1.4]
Systolic blood pressure, mmHg	110 [106–114.8]
Diastolic blood pressure, mmHg	60 [50–61.3]

Values are presented as median [interquartile range], unless otherwise indicated. **Abbreviations.** FiO_2, fraction of inspired oxygen; HCO_3^-, bicarbonate; IQR, interquartile range; PICU, pediatric intensive care unit; PIM2, Pediatric Index of Mortality 2; pSOFA, pediatric Sequential Organ Failure Assessment; $PvCO_2$, venous partial pressure of carbon dioxide; SpO_2, peripheral oxygen saturatio

Asynchrony Index and PVAs are summarized in Table 2 and Fig. 3.

Table 2
Patient–ventilator asynchronies across the three ventilator configurations.

Variable	SLC-Turbine	DLC-Turbine	DLC-PICU	Friedman p	Hodges–Lehmann paired difference (95% CI); p value
Asynchrony index, %	7.5 [0–13.7]	16.8 [7.6–25]	34.2 [17.4–67]	0.0001	Primary: DLC-PICU − SLC-Turbine: +33.0 (23.5 to 41.6); p = 0.0001 Secondary: DLC-PICU − DLC-Turbine: +24.2 (15.4 to 32.7); p = 0.0001 Exploratory: DLC-Turbine − SLC-Turbine: +8.5 (4.3 to 13.3); p = 0.0001
Ineffective efforts, n/min	0 [0–4]	0 [0–3]	0 [0–1]	0.090	—
Auto-triggering, n/min	0 [0–0]	2 [0–9.2]	4 [0–12.5]	0.0001	Primary: DLC-PICU − SLC-Turbine: +5 (2 to 7.5); p = 0.0001 Secondary: DLC-PICU − DLC-Turbine: 0 (− 3 to + 3); p = 0.947 Exploratory: DLC-Turbine − SLC-Turbine: +3.9 (2.3 to 7.4); p = 0.0001
Double triggering, n/min	0 [0–1]	0 [0–0]	0 [0–0]	0.022	Primary: DLC-PICU − SLC-Turbine: 0 (0 to 0); p = 0.506 Secondary: DLC-PICU − DLC-Turbine: 0 (− 1 to 0); p = 0.028 Exploratory: DLC-Turbine − SLC-Turbine: 0 (0 to + 0.5); p = 0.010
Premature cycling, n/min	1 [0.2–1.8]	1.1 [0.41–1.8]	1.8 [0.77–1.9]	0.671	—
Late cycling, n/min	0 [0–0]	0 [0–6]	0 [0–10]	0.0001	Primary: DLC-PICU − SLC-Turbine: +2.5 (0 to 8.5); p = 0.002 Secondary: DLC-PICU − DLC-Turbine: +1.0 (0 to 8); p = 0.070 Exploratory: DLC-Turbine − SLC-Turbine: +1.5 (0 to 3.5); p = 0.0001

Values are presented as median [interquartile range] and include all 12 infants; no recordings were excluded. Overall differences among the three ventilator configurations were assessed using the Friedman

test for repeated measures, followed by Wilcoxon signed-rank tests for predefined pairwise comparisons. Effect sizes are reported as Hodges-Lehmann median differences with 95% confidence intervals (CI). Differences are expressed as first-named minus second-named configuration; therefore, positive values indicate higher values in the first-named configuration. The primary endpoint was the difference in Asynchrony Index (AI) between DLC-PICU and SLC-Turbine, whereas the secondary endpoint compared DLC-PICU and DLC-Turbine. Comparisons between the two turbine configurations were prespecified as exploratory. No adjustment for multiple comparisons was applied; therefore, secondary and exploratory pairwise comparisons should be interpreted with caution. A dash (—) indicates that no pairwise comparison is reported because the overall Friedman test was not significant.

Abbreviations: CI, confidence interval; DLC-PICU, pediatric intensive care unit ventilator with dual-limb circuit; DLC-Turbine, turbine-driven ventilator with dual-limb circuit and active expiratory valve; IQR, interquartile range; SLC-Turbine, turbine-driven ventilator with single-limb circuit and intentional leak

Patient-ventilator asynchronies differed significantly across the three ventilator configurations (Table 2). The asynchrony index was lowest with SLC-Turbine (median 7.5% [IQR 0–13.7]), intermediate with DLC-Turbine (16.8% [7.6–25]), and highest with DLC-PICU (34.2% [17.4–67]; Friedman p = 0.0001). Pairwise comparisons using the Hodges-Lehmann estimator confirmed a significantly higher asynchrony index for DLC-PICU compared with SLC-Turbine (primary comparison: +33.0%; 95% CI 23.5 to 41.6; p = 0.0001) and compared with DLC-Turbine (secondary comparison: +24.2%; 95% CI 15.4 to 32.7; p = 0.0001). DLC-Turbine also showed a significantly higher asynchrony index than SLC-Turbine (exploratory comparison: +8.5%; 95% CI 4.3 to 13.3; p = 0.0001).

The rate of ineffective efforts did not differ significantly among the three configurations (0 [0–4], 0 [0–3], and 0 [0–1] events/min for SLC-Turbine, DLC-Turbine, and DLC-PICU, respectively; p = 0.090).

Auto-triggering was significantly more frequent with DLC-PICU than with SLC-Turbine (4 [0–12.5] vs 0 [0–0] events/min; primary comparison: +5 events/min, 95% CI 2 to 7.5; p = 0.0001) and than with DLC-Turbine in the exploratory comparison (+ 3.9 events/min; 95% CI 2.3 to 7.4; p = 0.0001).

No significant difference was observed between DLC-PICU and DLC-Turbine (secondary comparison: 0 events/min, 95% CI − 3 to + 3; p = 0.947), whereas auto-triggering was more frequent with DLC-Turbine than with SLC-Turbine in the exploratory comparison (+ 3.9 events/min, 95% CI 2.3 to 7.4; p = 0.0001).

Double triggering showed a small but statistically significant overall difference across configurations (p = 0.022). No significant difference was observed for the primary comparison (DLC-PICU vs SLC-Turbine: 0; 95% CI 0 to 0; p = 0.506), while both the secondary comparison (DLC-PICU vs DLC-Turbine: 0; 95% CI − 1 to 0; p = 0.028) and the exploratory comparison (DLC-Turbine vs SLC-Turbine: 0; 95% CI 0 to 0.5; p = 0.010) reached statistical significance.

Premature cycling did not differ significantly among the three configurations (p = 0.671).

Late cycling occurred significantly more often with DLC-PICU than with SLC-Turbine (0 [0–0] vs 0 [0–10] events/min; primary comparison: +2.5 events/min; 95% CI 0 to 8.5; p = 0.002) and was significantly higher

with DLC-Turbine than with SLC-Turbine in the exploratory comparison (+ 1.5 events/min; 95% CI 0 to 3.5; p = 0.0001), while the difference between DLC-PICU and DLC-Turbine did not reach statistical significance (secondary comparison: +1.0 events/min; 95% CI 0 to 8; p = 0.070).

Breathing pattern, ventilatory mechanics, and patient–ventilator timings are reported in Table 3 and Fig. 4.

Table 3
Breathing pattern, ventilatory mechanics and patient–ventilator timings.

Variable	Spontaneous breathing	SLC-Turbine	DLC-Turbine	DLC-PICU	Friedman p	HL difference (95% CI); p value
Ventilatory mechanics						
Peak airway pressure, cmH_2O	—	11 [11–14]	11 [10–14]	10.5 [10–12.7]	0.415	—
Rise time, ms	—	339 [273–362]	297 [233–343]	245 [174–386]	0.242	—
Peak inspiratory flow, mL/s	—	613 [445–774]	730 [504–806]	760 [709–992]	0.148	—
PEEP, cmH_2O	—	5 [5–7]	5 [5–5.8]	5 [5–5.7]	0.711	—
Respiratory effort and breathing pattern						
ΔPes, cmH_2O	16 [10–26]	7.6 [5–12.7]	5 [4.5–10]	7 [5–9.7]	0.0001	SLC-Turbine vs SB: −13 (− 26 to − 4); p = 0.004 DLC-Turbine vs SB: −13.3 (− 25.5 to − 4.5); p = 0.039 DLC-PICU vs SB: −13.5 (− 26 to − 2.5); p = 0.001 DLC-Turbine vs SLC-Turbine: −0.51 (− 3.6 to + 2.5); p = 0.688 SLC-Turbine vs DLC-PICU: +0.75 (− 2.5 to +

Variable	Spontaneous breathing	SLC-Turbine	DLC-Turbine	DLC-PICU	Friedman p	HL difference (95% CI); p value
Ventilatory mechanics						
						4); p = 0.540 DLC-PICU vs DLC-Turbine: +0.5 (−0.75 to + 3.75); p = 0.342

Variable	Spontaneous breathing	SLC-Turbine	DLC-Turbine	DLC-PICU	Friedman p	HL difference (95% CI); p value
Ventilatory mechanics						
PTPes, $cmH_2O \cdot s \cdot min^{-1}$	534 [318–648]	180 [117–394]	134 [99–08]	135 [101–278]	0.0001	SLC-Turbine vs SB: −256 (− 412 to − 103); p = 0.004 DLC-Turbine vs SB: −330 (− 520 to − 161); p = 0.002 DLC-PICU vs SB: −307 (− 481 to − 92); p = 0.004 DLC-Turbine vs SLC-Turbine: −53 (− 168 to + 20); p = 0.240 SLC-Turbine vs DLC-PICU: +6.2 (− 116 to + 69); p = 0.898 DLC-PICU vs DLC-Turbine: +47 (− 47 to + 174); p = 0.101
Patient respiratory rate, breaths/min	50 [45–56]	36 [32–38]	31 [26–33]	38 [31–42]	0.001	SLC-Turbine vs SB: −19 (− 31 to − 4); p = 0.001 DLC-Turbine vs

Variable	Spontaneous breathing	SLC-Turbine	DLC-Turbine	DLC-PICU	Friedman p	HL difference (95% CI); p value
Ventilatory mechanics						
						SB: −16 (− 27 to − 7); p = 0.01 DLC-PICU vs SB: −18 (− 27 to − 11); p = 0.001 DLC-Turbine vs SLC-Turbine: −5 (− 9 to − 3); p = 0.01 DLC-PICU vs SLC-Turbine: +1.5 (− 1 to + 3.5); p = 0.264 DLC-PICU vs DLC-Turbine: +7 (+ 4.5 to + 10); p = 0.0001
Ventilator respiratory rate, breaths/min	—	33 [29–44]	30 [25–48]	48 [4-53]	0.001	DLC-PICU vs SLC-Turbine: +9 (+ 6 to + 13); p = 0.001 DLC-PICU vs DLC-Turbine: +12 (+ 8 to + 16); p = 0.001 SLC-Turbine vs DLC-Turbine: +5 (− 6.5 to + 17); p = 0.359

Variable	Spontaneous breathing	SLC-Turbine	DLC-Turbine	DLC-PICU	Friedman p	HL difference (95% CI); p value
Ventilatory mechanics						
Patient Ti/Ttot	0.51 [0.47–0.55]	0.50 [0.43–0.59]	0.49 [0.42–0.59]	0.51 [0.41–0.57]	0.260	—
Ventilator Ti/Ttot	—	0.41 [0.31–0.50]	0.43 [0.35–0.51]	0.58 [0.48–0.66]	0.357	—
Patient–ventilator timing and synchrony						
Inspiratory time, patient, ms	452 [352– 604]	466 [336–573]	378 [312–529]	423 [397–512]	0.634	—
Inspiratory time, ventilator, ms	—	458 [436–553]	389 [346–523]	418 [374–470]	0.320	—
Expiratory time, patient, ms	373 [316–424]	538 [386–596]	488 [307–800]	670 [483–775]	0.008	SLC-Turbine vs SB: +133 (+ 91 to + 389); p = 0.003 DLC-Turbine vs SB: +166 (− 53 to + 389); p = 0.164 DLC-PICU vs SB: +296 (+ 186 to + 370); p = 0.003 SLC-Turbine vs DLC-Turbine: +42 (− 105 to + 263); p = 0.563 DLC-PICU vs SLC-Turbine: +157 (− 70 to + 285); p = 0.101

Variable	Spontaneous breathing	SLC-Turbine	DLC-Turbine	DLC-PICU	Friedman p	HL difference (95% CI); p value
Ventilatory mechanics						
						DLC-PICU vs DLC-Turbine: +176 (+ 43 to + 309); p = 0.009
Expiratory time, ventilator, ms	—	673 [500–800]	455 [313–1000]	455 [361–1249]	0.351	—
Inspiratory delay, ms	—	215 [178–399]	209 [147–263]	168 [119–342]	0.920	—
Expiratory delay, ms	—	256 [207–348]	311 [246–541]	310 [215–531]	0.461	—
Synchronization time, % of inspiratory time	—	45 [29.7–62.5]	42 [28.3–55]	39.5 [32.1–54.6]	0.07	—

Values are presented as median [interquartile range] and include all 12 infants; no recordings were excluded. Variables measurable during spontaneous breathing were compared across all four conditions (SB, SLC-Turbine, DLC-Turbine, and DLC-PICU), whereas ventilator-dependent variables were compared across the three ventilator configurations only. Overall differences were assessed using the Friedman test, followed by Wilcoxon signed-rank tests for pairwise comparisons. Effect sizes are reported as Hodges-Lehmann median differences with 95% confidence intervals (CI). Differences are expressed as first-named minus second-named condition. No adjustment for multiple comparisons was applied. A dash (—) indicates that the variable was not applicable or that the overall Friedman test was not significant.

Abbreviations: CI, confidence interval; DLC-PICU, pediatric intensive care unit ventilator with dual-limb circuit; DLC-Turbine, turbine-driven ventilator with dual-limb circuit and active expiratory valve; IQR, interquartile range; PEEP, positive end-expiratory pressure; PTPes, esophageal pressure–time product; SB, spontaneous breathing; SLC-Turbine, turbine-driven ventilator with single-limb circuit and intentional leak; Ti/Ttot, ratio of inspiratory time to total respiratory cycle time; ΔPes, esophageal pressure swing

Ventilatory mechanics did not differ across the three ventilator configurations. Peak airway pressure (11 [11–14] vs 11 [10–14] vs 10.5 [10–12.7] cmH_2O for SLC-Turbine, DLC-Turbine, and DLC-PICU, respectively), rise time (339 [273–362] vs 297 [233–343] vs 245 [174–386] ms), peak inspiratory flow (613 [445–774] vs 730 [504–806] vs 760 [709–992] mL/s), and PEEP (5 [5.0–7] vs 5 [5–5.8] vs 5.0 [5–5.7] cmH_2O) were all similar (all $p > 0.14$).

Respiratory effort and breathing pattern changed with ventilation compared with spontaneous breathing. Esophageal pressure swing (ΔPes) was 16 [10–26] cmH_2O during spontaneous breathing versus 7.6 [5–

12.7] cmH_2O with SLC-Turbine, 5 [4.5–10] cmH_2O with DLC-Turbine, and 7 [5–9.7] cmH_2O with DLC-PICU (overall p = 0.0001); the reduction from spontaneous breathing was significant for all three configurations (SLC-Turbine: −13 cmH_2O, 95% CI − 26 to − 4, p = 0.004; DLC-Turbine: −13.3 cmH_2O, 95% CI − 25.5 to − 4.5, p = 0.039; DLC-PICU: −13.5 cmH_2O, 95% CI − 26 to − 2.5, p = 0.001). The esophageal pressure–time product (PTPes) showed the same pattern: 534 [318–648] $cmH_2O{\cdot}s{\cdot}min^{-1}$ during spontaneous breathing versus 180 [117–394], 134 [99–308], and 135 [101–278] $cmH_2O{\cdot}s{\cdot}min^{-1}$ with SLC-Turbine, DLC-Turbine, and DLC-PICU, respectively (overall p = 0.0001; SLC-Turbine vs spontaneous breathing: −256, 95% CI − 412 to − 103, p = 0.004; DLC-Turbine vs spontaneous breathing: −330, 95% CI − 520 to − 161, p = 0.002; DLC-PICU vs spontaneous breathing: −307, 95% CI − 481 to − 92, p = 0.004). In contrast, neither variable differed between the ventilator configurations: SLC-Turbine vs DLC-PICU (ΔPes: HL + 0.75 cmH_2O, 95% CI − 2.5 to + 4, p = 0.540; PTPes: HL + 6.2 $cmH_2O{\cdot}s{\cdot}min^{-1}$, 95% CI − 116 to + 69, p = 0.898) and DLC-Turbine vs SLC-Turbine (ΔPes: HL − 0.51 cmH_2O, 95% CI − 3.6 to + 2.5, p = 0.688; PTPes: HL − 53 $cmH_2O{\cdot}s{\cdot}min^{-1}$, 95% CI − 168 to + 20, p = 0.240).

Patient respiratory rate fell from 50 [45–56] breaths/min during spontaneous breathing to 36 [32–38], 31 [26–33], and 38 [31–42] breaths/min with SLC-Turbine, DLC-Turbine, and DLC-PICU, respectively (overall p = 0.001; SLC-Turbine vs spontaneous breathing: −19 breaths/min, 95% CI − 31 to − 4, p = 0.001; DLC-Turbine vs spontaneous breathing: −16 breaths/min, 95% CI − 27 to − 7, p = 0.01; DLC-PICU vs spontaneous breathing: −18 breaths/min, 95% CI − 27 to − 11, p = 0.001). Patient respiratory rate also differed between ventilator configurations: it was lower with DLC-Turbine than with SLC-Turbine (− 5 breaths/min, 95% CI − 9 to − 3, p = 0.01) and higher with DLC-PICU than with DLC-Turbine (+ 7 breaths/min, 95% CI + 4.5 to + 10, p = 0.0001), whereas DLC-PICU and SLC-Turbine did not differ (+ 1.5 breaths/min, 95% CI − 1 to + 3.5, p = 0.264). Ventilator respiratory rate, in contrast, was higher with DLC-PICU (48 [43–53] breaths/min) than with SLC-Turbine (33 [29–44] breaths/min; +9 breaths/min, 95% CI + 6 to + 13, p = 0.001) or DLC-Turbine (30 [25–48] breaths/min; +12 breaths/min, 95% CI + 8 to + 16, p = 0.001), whereas SLC-Turbine and DLC-Turbine did not differ (+ 5 breaths/min, 95% CI − 6.5 to + 17, p = 0.359). Patient Ti/Ttot did not differ across conditions (0.51 [0.47–0.55] vs 0.50 [0.43–0.59] vs 0.49 [0.42–0.59] vs 0.51 [0.41–0.57]; p = 0.260), nor did ventilator Ti/Ttot (p = 0.357).

Patient–ventilator timing showed condition-dependent differences confined to the respiratory cycle of the patient. Patient inspiratory time was similar across the three configurations. Patient expiratory time was 373 [316–424] ms during spontaneous breathing versus 538 [386–596], 488 [307–800], and 670 [483–775] ms with SLC-Turbine, DLC-Turbine, and DLC-PICU, respectively (overall p = 0.008), and was longer with DLC-PICU than during spontaneous breathing (+ 296 ms, 95% CI + 186 to + 370, p = 0.003). Expiratory time was also longer with SLC-Turbine than during spontaneous breathing (spontaneous breathing vs SLC-Turbine: +133 ms, 95% CI + 91 to + 398, p = 0.003) and longer with DLC-PICU than with DLC-Turbine (+ 176 ms, 95% CI + 43 to + 309, p = 0.009); no other pairwise comparison of patient inspiratory or expiratory time reached significance. Ventilator-side inspiratory and expiratory time, inspiratory and expiratory delay, and the proportion of inspiratory time spent synchronized did not differ across the three ventilator configurations (all $p \geq 0.07$).

Discussion

In this randomized physiological crossover study, we found that turbine-driven ventilators substantially improved patient–ventilator interaction during NIV in infants with acute respiratory failure compared with a conventional dual-limb compressed-gas pediatric ICU ventilator. Both turbine configurations reduced the burden of patient–ventilator asynchrony, whereas the intentional-leak single-limb configuration achieved the lowest Asynchrony Index. Importantly, these marked improvements in synchrony occurred without measurable differences in respiratory muscle unloading. Together, these findings indicate that synchrony and inspiratory effort represent complementary, rather than interchangeable, physiological dimensions of NIV performance.

As NIV is increasingly adopted not only in PICUs but also in pediatric wards, emergency departments, transport medicine, and home-care settings, optimizing patient–ventilator interaction has become progressively more relevant for clinical practice [6, 8, 28, 41]. Previous pediatric physiological studies have consistently shown that patient–ventilator asynchrony remains common during NIV despite careful optimization of ventilator settings [6–8, 28, 34, 36]. Achieving synchrony is particularly challenging in infants because of their small tidal volumes, short neural inspiratory times, weak inspiratory efforts, and rapidly changing interface leaks, all of which interfere with trigger detection and cycling performance [28]. Against this background, our findings demonstrate that ventilator technology has a major influence on patient–ventilator interaction under real clinical conditions.

The superior synchrony observed with the turbine-driven ventilators is physiologically plausible and consistent with previous experimental and clinical evidence in adults [4]. Dedicated turbine-driven NIV ventilators have been specifically developed to operate under conditions of variable leak, incorporating adaptive triggering, cycling, and leak-compensation algorithms that continuously adjust ventilator performance [4, 9, 31–33]. Bench studies have consistently demonstrated substantial inter-device variability in leak compensation and trigger performance, particularly under dynamic leak conditions that closely resemble pediatric NIV [31–35, 39, 40]. Likewise, Carteaux and colleagues showed in adults that dedicated NIV ventilators provided better synchrony than conventional ICU ventilators despite active leak-compensation algorithms [4]. Our findings extend these observations to infants, suggesting that these technological differences remain clinically relevant even in the most challenging physiological setting.

A particularly novel aspect of the present study is the comparison between the two turbine-driven configurations, which partially separates the contribution of ventilator technology from that of circuit architecture. To our knowledge, this is the first physiological study evaluating these components independently during pediatric NIV. Although both turbine configurations outperformed the compressed-gas ICU ventilator, synchrony was consistently superior with the intentional-leak single-limb circuit. Because the ventilator platform was identical, these findings suggest that circuit architecture contributes independently to patient–ventilator interaction. An intentional-leak circuit forms an integral part of the ventilator's leak-management strategy, whereas dual-limb circuits require continuous discrimination between patient-generated flow, unintentional leaks, and valve operation. Previous bench studies suggested that circuit configuration influences trigger performance and leak compensation [9, 31–35], whereas our results demonstrate that these physiological differences are also evident in infants NIV. Rather than identifying a

single determinant of synchrony, our findings support the concept that optimal patient–ventilator interaction results from the integration of ventilator platform, circuit design, and adaptive control algorithms.

Another important observation is that the reduction in overall asynchrony was primarily driven by near elimination of auto-triggering together with a marked reduction in late cycling, whereas ineffective efforts remained infrequent across all configurations. These findings suggest that ventilators generate distinct asynchrony phenotypes, rather than simply different quantities of asynchronous events. An Asynchrony Index dominated by auto-triggering is physiologically different from one characterized by ineffective efforts or double triggering, and these patterns are unlikely to carry identical clinical implications [5–7, 34, 36]. Future physiological studies should therefore characterize not only the overall burden of asynchrony but also its predominant phenotype.

Perhaps the most clinically relevant finding of this study is the clear dissociation between patient–ventilator synchrony and respiratory muscle unloading. Despite an approximately four-fold reduction in the Asynchrony Index, esophageal pressure swing and esophageal pressure–time product were remarkably similar among the three ventilator configurations. Respiratory effort depends on multiple physiological determinants, including respiratory drive, pressure support, lung mechanics, and neural control of breathing, in addition to patient–ventilator synchrony [27, 36–38]. Consequently, the Asynchrony Index should not be interpreted as a surrogate measure of inspiratory effort. This concept is particularly relevant in the current era of lung- and diaphragm-protective ventilation, where optimization of respiratory support increasingly requires simultaneous assessment of synchrony, respiratory drive, and inspiratory effort rather than reliance on any single physiological variable [37, 38].

Our findings may also help explain why the relationship between patient–ventilator asynchrony and clinical outcomes has appeared less consistent in pediatric than in adult studies. In adults, high asynchrony burdens have been associated with prolonged ventilation and increased mortality [5]. Pediatric investigations, however, have reported weaker and sometimes inconsistent associations [41]. Our results suggest that these discrepancies may reflect differences in the predominant type of asynchronous events rather than the absolute Asynchrony Index alone. Auto-triggering, for example, increases ventilator respiratory rate without necessarily increasing respiratory muscle workload, whereas ineffective efforts directly reduce effective ventilatory assistance and increase the work required to trigger the ventilator [36]. These observations reinforce the need to interpret the Asynchrony Index together with respiratory effort and the specific pattern of asynchronous events.

The present findings also have practical implications: the ability of dedicated turbine-driven ventilators to provide effective NIV without a compressed-gas source may facilitate respiratory support during transport, emergency care, pediatric high-dependency units, and other settings where compressed-gas infrastructure is unavailable or limited. Whether the physiological advantages demonstrated here translate into improved comfort, lower NIV failure rates, or better clinical outcomes deserves investigation in adequately powered clinical trials.

Our study has several strengths. The randomized crossover design allowed each infant to serve as his or her own control, minimizing the influence of interindividual variability in respiratory mechanics, disease

severity, respiratory drive, and interface fit. Ventilator settings, sedation, body position, and interface were maintained constant throughout the study, while esophageal manometry provided direct assessment of inspiratory effort and neural respiratory timing, allowing simultaneous evaluation of patient–ventilator interaction and respiratory muscle unloading.

Several limitations should be acknowledged. This was a single-center physiological study involving a relatively small number of patients and short observation periods; therefore, it was not designed to evaluate clinically relevant outcomes such as NIV failure, intubation, or duration of respiratory support. Only one representative ventilator from each technological platform was evaluated, and trigger, cycling, and leak-compensation algorithms differ substantially across manufacturers [31–35]. Finally, although the comparison between the two turbine configurations provides important physiological insight into the contribution of circuit architecture, the individual effects of hardware and proprietary software algorithms cannot be completely separated. Moreover, tidal volume and leak could not be compared reliably across configurations. With dual-limb systems, expiratory leaks may compromise the accuracy of exhaled tidal-volume measurements in children. With turbine-driven systems, dynamic unintentional leaks may affect algorithm-based tidal-volume estimates. Therefore, these measurements could not be reliably compared between configurations and were therefore not considered study outcomes.

Conclusions

Turbine-driven ventilators improved patient–ventilator interaction compared with a conventional dual-limb compressed-gas pediatric ICU ventilator during NIV in infants with acute respiratory failure. The lowest asynchrony burden was observed with the intentional-leak single-limb configuration, suggesting that patient–ventilator interaction is influenced by the combined effects of ventilator platform, circuit architecture, and leak-compensation algorithms. These improvements in synchrony were not accompanied by measurable differences in inspiratory effort. Beyond its physiological advantages, the single-limb turbine-driven configuration offers practical benefits, including portability, independence from compressed-gas sources, and ease of deployment, making it particularly attractive for emergency departments, interhospital transport, pediatric high-dependency units, and resource-limited settings where timely delivery of effective NIV is essential. Whether these physiological advantages translate into improved patient comfort, lower NIV failure rates, or better clinical outcomes should be evaluated in future adequately powered clinical trials.

Abbreviations

AI
asynchrony index
CI
confidence interval
COMFORT
Comfort Behavior Scale
DLC-PICU
dual-limb circuit with intensive care unit ventilator configuration

DLC-Turbine
dual-limb circuit with turbine-driven ventilator configuration
FiO_2
fraction of inspired oxygen
HL
Hodges–Lehmann
IQR
interquartile range
NIV
noninvasive ventilation
PEEP
positive end-expiratory pressure
Pes
esophageal pressure
ΔPes
esophageal pressure swing
PICU
pediatric intensive care unit
PIM2
Pediatric Index of Mortality 2
pSOFA
pediatric Sequential Organ Failure Assessment
PS
pressure support
PTPes
esophageal pressure–time product
RR
respiratory rate
SB
spontaneous breathing
SLC-Turbine
single-limb circuit with turbine-driven ventilator configuration
SpO_2
peripheral oxygen saturation.

Declarations

Ethics approval and consent to participate.

The study protocol was approved by the Comitato Etico Milano Area 2 (approval 600_2019bis, 18 June 2019). Written informed consent was obtained from the parents or legal guardians of all participants.

Consent for publication.

Not applicable.

Availability of data and materials.

The datasets generated and analysed during the current study are available from the corresponding author on reasonable request.

Competing interests.

The Authors declare that they have no competing interests.

Funding.

The study did not reveived specifica funding.

Authors’ contributions.

All authors fulfill the authorship criteria established by the International Committee of Medical Journal Editors (ICMJE). Giovanna Chidini, Domenico Luca Grieco and Cesare Gregoretti contribute equally to the conception and design of the study, the acquisition, analysis and interpretation of data, and drafted and critically revised the manuscript for important intellectual content. Edoardo Calderini, who mentored this study, contributed to its conception and design. Thomas Langer, Cristina Villa, Stefano Scalia Catenacci, Tiziana Marchesi, Maria Francesca Patria and Giacomo Grasselli contribute to the acquisition, analysis and interpretation of data, and drafted or critically revised the manuscript for important intellectual content. All authors approved the final version of the manuscript and agree to be accountable for all aspects of the work, including ensuring that questions related to the accuracy or integrity of any part of the work are appropriately investigated and resolved.

Reporting Guidelines

This manuscript has not been published previously and is not under consideration elsewhere. All authors have approved the manuscript and agree with its submission. The study was conducted in accordance with institutional ethical standards and the Declaration of Helsinki and was reported following the CONSORT reporting guidelines for randomized trials and the recommendations of the EQUATOR Network.

Acknowledgements

The Authors thank the nursing and respiratory therapy staff of the Pediatric Intensive Care Unit, Fondazione IRCCS Ca' Granda Ospedale Maggiore Policlinico, for their assistance throughout data collection, and the families of the participating infants for their trust and collaboration in this study.

The authors wish to honor the memory of Edoardo Calderini, MD, co-author of this work, who passed away during its preparation. His contribution to the design of this study and to pediatric intensive care research is gratefully acknowledged.

AI Disclosure

Artificial intelligence (AI)-assisted tools were used solely for language editing and stylistic revision. All scientific content, analyses, interpretations, and conclusions were developed, critically reviewed, and approved by the authors. The authors retain full intellectual ownership of the manuscript and assume complete responsibility for its content.

References

1. Rochwerg B, Brochard L, Elliott MW, et al. Official ERS/ATS clinical practice guidelines: noninvasive ventilation for acute respiratory failure. Eur Respir J. 2017;50:1602426.
2. Carroll CL, Napolitano N, Pons-Òdena M et al. Noninvasive respiratory support for pediatric acute respiratory distress syndrome: From the Second Pediatric Acute Lung Injury Consensus Conference. Pediatr Crit Care Med. 2023;24(Suppl 2):S135–S147.
3. Kneyber MCJ, de Luca D, Calderini E et al. Recommendations for mechanical ventilation of critically ill children from the Paediatric Mechanical Ventilation Consensus Conference (PEMVECC). Intensive Care Med. 2017;43:1764–1780.
4. Carteaux G, Lyazidi A, Cordoba-Izquierdo A, et al. Patient–ventilator asynchrony during noninvasive ventilation: a bench and clinical study. Chest. 2012;142(2):367–76.
5. Blanch L, Villagra A, Sales B, et al. Asynchronies during mechanical ventilation are associated with mortality. Intensive Care Med. 2015;41:633–41.
6. Ducharme-Crevier L, Beck J, Essouri S, et al. Neurally adjusted ventilatory assist allows patient–ventilator synchrony during pediatric noninvasive ventilation: a crossover physiological study. Crit Care. 2015;19:44.
7. Thille AW, Rodriguez P, Cabello B, et al. Patient–ventilator asynchrony during assisted mechanical ventilation. Intensive Care Med. 2006;32:1515–22.
8. Chidini G, De Luca D, Conti G, et al. Early noninvasive neurally adjusted ventilatory assist versus pressure support ventilation in pediatric acute respiratory failure. Pediatr Crit Care Med. 2016;17:e487–95.
9. Carlucci A, Schreiber A, Mattei A, et al. Configuration of bilevel ventilator circuits affects compensation for nonintentional leaks during volume-targeted ventilation. Intensive Care Med. 2013;39:59–65.
10. Khirani S, Stehling F, Dudoignon B, et al. Trigger issues with a life support device in children. Sleep Med. 2025;131:106534.
11. Khirani S, Louis B, Leroux K, et al. Improvement of ventilator triggering during noninvasive ventilation in children: bench and clinical study. Clin Respir J. 2016;10:559–66.
12. Calderini E, Confalonieri PG, Puccio P, Francavilla N, Stella L, Gregoretti C. Patient–ventilator asynchrony during noninvasive ventilation: role of the expiratory trigger. Intensive Care Med. 1999;25:662–7.
13. MacLean JE, Fauroux B. Long-term noninvasive ventilation in children: transition from hospital to home. Paediatr Respir Rev. 2023;47:3–10.

14. Gregoretti C, Navalesi P, Ghannadian S, et al. Choosing a ventilator for home mechanical ventilation. Breathe (Sheff). 2013;9:394–409.
15. Esposito I, Chatwin M, Accurso G, et al. Ventilator configuration in children on long-term home ventilation during the COVID-19 pandemic. Pulmonology. 2021;27:448–52.
16. Begg C, Cho M, Eastwood S, et al. Improving the quality of reporting of randomized controlled trials: the CONSORT statement. JAMA. 1996;276:637–9.
17. Mathers LH, Frankel LR. Stabilization of the critically ill child. In: Behrman RE, Kliegman RM, Jenson HB, editors. Nelson Textbook of Pediatrics. 17th ed. Philadelphia: Saunders; 2004. pp. 387–419.
18. WHO Multicentre Growth Reference Study Group. WHO child growth standards based on length/height, weight and age. Acta Paediatr Suppl. 2006;450:76–85.
19. Bernet V, Hug MI, Frey B. Predictive factors for success of noninvasive mask ventilation in infants and children with acute respiratory failure. Pediatr Crit Care Med. 2005;6:660–4.
20. Colombo D, Cammarota G, Bergamaschi V, et al. Physiologic response to varying levels of pressure support and neurally adjusted ventilatory assist in acute respiratory failure. Intensive Care Med. 2008;34:2010–8.
21. Conti G, Gregoretti C, Spinazzola G, et al. Influence of different interfaces on synchrony during pressure support ventilation in a pediatric setting: a bench study. Respir Care. 2015;60:498–507.
22. Ambuel B, Hamlett KW, Marx CM, et al. Assessing distress in pediatric intensive care environments: the COMFORT scale. J Pediatr Psychol. 1992;17:95–109.
23. Venn RM, Hell J, Grounds RM. Respiratory effects of dexmedetomidine in the surgical patient requiring intensive care. Crit Care. 2000;4:302–8.
24. Hotz JC, Sodetani CT, Van Steenbergen J, et al. Esophageal balloon filling volume affects measurements in children with ARDS. Respir Care. 2018;63:177–86.
25. Mauri T, Alban L, Turrini C, et al. Optimum support by high-flow nasal cannula in acute hypoxemic respiratory failure. Intensive Care Med. 2017;43:1453–63.
26. Chiumello D, Chidini G, Calderini E, et al. Respiratory mechanics and lung stress/strain in children with acute respiratory distress syndrome. Ann Intensive Care. 2016;6:11.
27. Tonelli R, Fantini R, Tabbì L, et al. Early inspiratory effort assessment by esophageal manometry predicts noninvasive ventilation outcome in de novo respiratory failure. A pilot study. Am J Respir Crit Care Med. 2020;202(4):558–67.
28. Vignaux L, Grazioli S, Piquilloud L, et al. Optimizing patient-ventilator synchrony during invasive ventilatory assist in children and infants remains a difficult task. Pediatr Crit Care Med. 2013;14:e316–25.
29. Hess DR. Patient–ventilator interaction during noninvasive ventilation. Respir Care. 2011;56(2):153–67.
30. Moon K, Takeuchi M, Tachibana K, et al. Accuracy of reported tidal volume during neonatal ventilation with airway leak: a lung model study. Pediatr Crit Care Med. 2019;20(1):e37–45.
31. Oto J, Chenelle CT, Marchese AD, et al. A comparison of leak compensation during pediatric noninvasive ventilation: a lung model study. Respir Care. 2013;58(12):2027–37.

32. Baumgartner J, Schmidt J, Klotz D, Schneider H, Schumann S, Fuchs H. Trigger performance of five pediatric home ventilators and one ICU ventilator depending on circuit type and system leak in a physical model of the lung. Pediatr Pulmonol. 2022;57(3):744–53.
33. Martínez-Castro S, Belda Nacher FJ, Puig Bernabeu J, Soro Domingo MB, Delgado Navarro C, Ortega Pons H. Are all ventilators for NIV performing the same? A bench analysis. J Clin Monit Comput. 2023;37(6):1497–511.
34. Mortamet G, Larouche A, Ducharme-Crevier L, et al. Patient-ventilator asynchrony during conventional mechanical ventilation in children. Ann Intensive Care. 2017;7(1):122.
35. Itagaki T, Chenelle CT, Bennett DJ, Fisher DF, Kacmarek RM. Effects of leak compensation on patient-ventilator synchrony during premature/neonatal invasive and noninvasive ventilation: a lung model study. Respir Care. 2017;62(1):22–33.
36. Blokpoel RGT, Koopman AA, van Dijk J, Kneyber MCJ. Additional work of breathing from trigger errors in mechanically ventilated children. Respir Res. 2020;21(1):296.
37. Khemani RG, Bhalla A, Hotz JC et al. Randomized Trial of Lung and Diaphragm Protective Ventilation in Children (REDvent). NEJM Evid 2025 (10.1056/EVIDoa2400360).
38. Vedrenne-Cloquet M, Ito Y, Hotz J, et al. Phenotypes based on respiratory drive and effort to identify the risk factors when P0.1 fails to estimate ΔPES in ventilated children. Crit Care. 2024;28(1):325.
39. Sogo A, Montanyà J, Monsó E, Blanch L, Pomares X, Lujàn M. Effect of dynamic random leaks on the monitoring accuracy of home mechanical ventilators: a bench study. BMC Pulm Med. 2013;13:75. 10.1186/1471-2466-13-75.
40. Chen Y, Cheng K, Zhou X. Effectiveness of Inspiratory Termination Synchrony with Automatic Cycling During Noninvasive Pressure Support Ventilation. Med Sci Monit. 2016;22:1694–701.
41. Blokpoel RGT, Burgerhof JGM, Markhorst DG, Kneyber MCJ. Trends in pediatric patient-ventilator asynchrony during invasive mechanical ventilation. Pediatr Crit Care Med. 2021;22(11):993–7. 10.1097/PCC.0000000000002788.

Figures

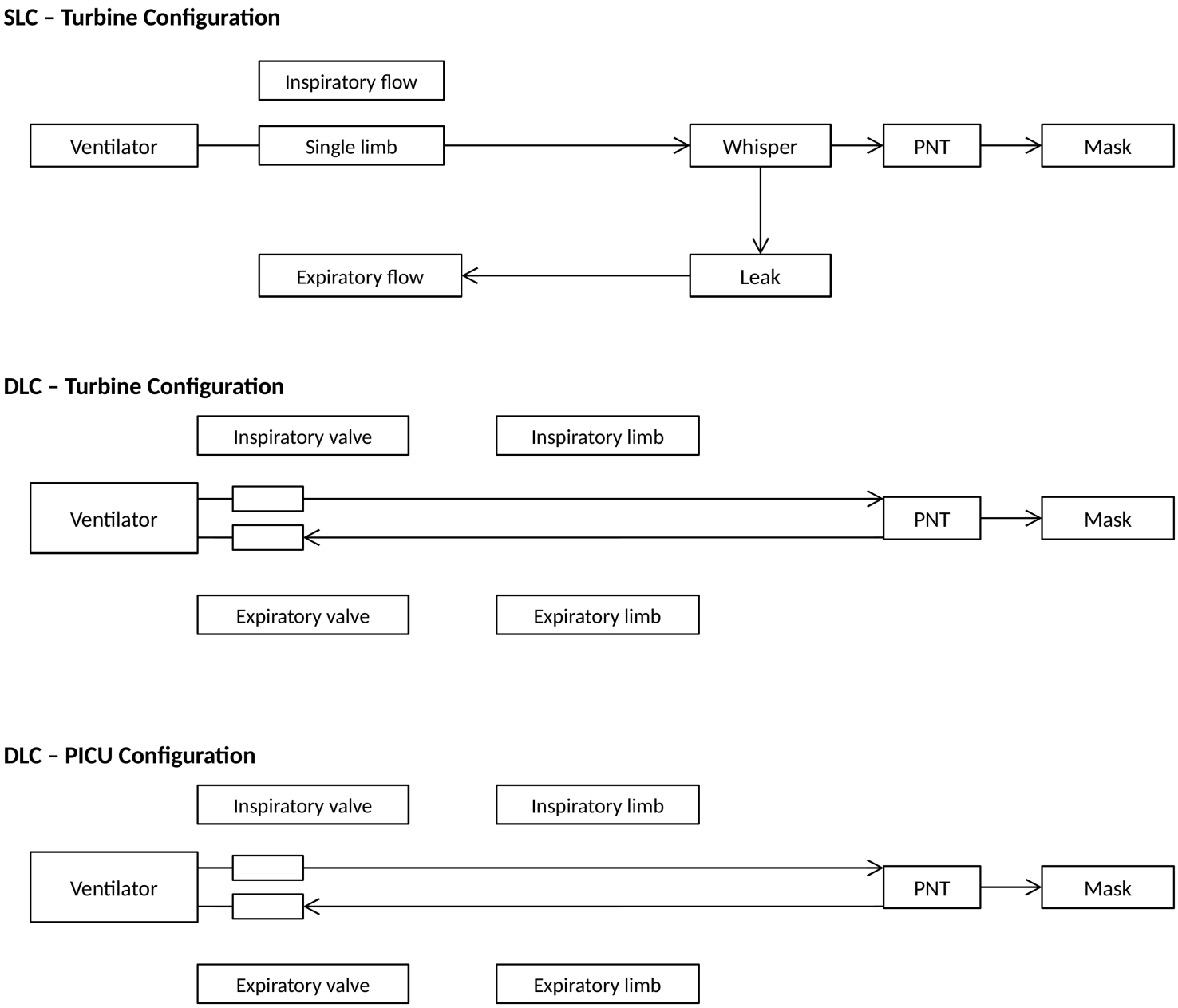


Figure 1

Non-invasive ventilation circuit configurations.

Schematic representation of the three ventilator configurations evaluated in the crossover protocol. Top: SLC-Turbine, a turbine-driven ventilator (Astral 150, ResMed) with a single-limb circuit and intentional leak through a Whisper valve. Middle: DLC-Turbine, the same ventilator configured with a dual-limb circuit and an active expiratory valve, isolating the effect of circuit configuration. Bottom: DLC-PICU, a dual-limb compressed-gas pediatric ICU ventilator (Babylog VN500, Dräger) with an active expiratory valve. Arrows indicate inspiratory and expiratory flow. PNT, pneumotachograph

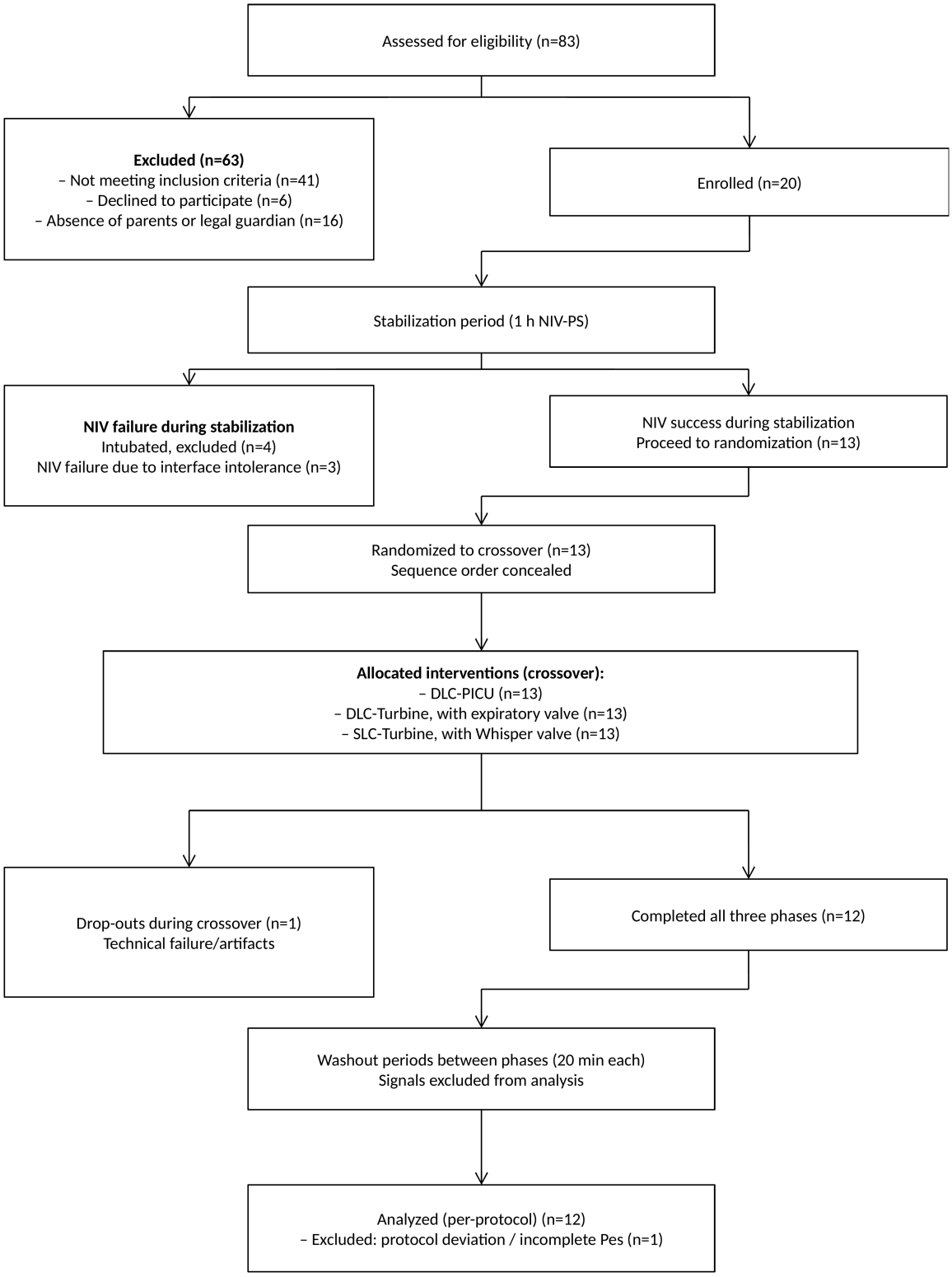


Figure 2

CONSORT flow diagram.

Flow of participants through screening, enrollment, randomization, and analysis. Of 83 infants assessed for eligibility, 63 were excluded and 20 were enrolled. Seven infants met predefined NIV failure criteria during the stabilization period and were intubated or excluded for interface intolerance; 13 infants met NIV

success criteria and were randomized to the three-condition crossover (allocated interventions: DLC-PICU, DLC-Turbine, and SLC-Turbine, each n=13). One infant was withdrawn during the crossover because of technical failure/artifacts; 12 infants completed all three phases and were analyzed per protocol. Abbreviations**.**NIV, noninvasive ventilation; PS, Pressure Support; PICU, pediatric intensive care unit; DLC-PICU, pediatric intensive care unit ventilator with dual-limb circuit; DLC-Turbine, turbine-driven ventilator with dual-limb circuit and active expiratory valve; SLC-Turbine, turbine-driven ventilator with single-limb circuit and intentional leak.

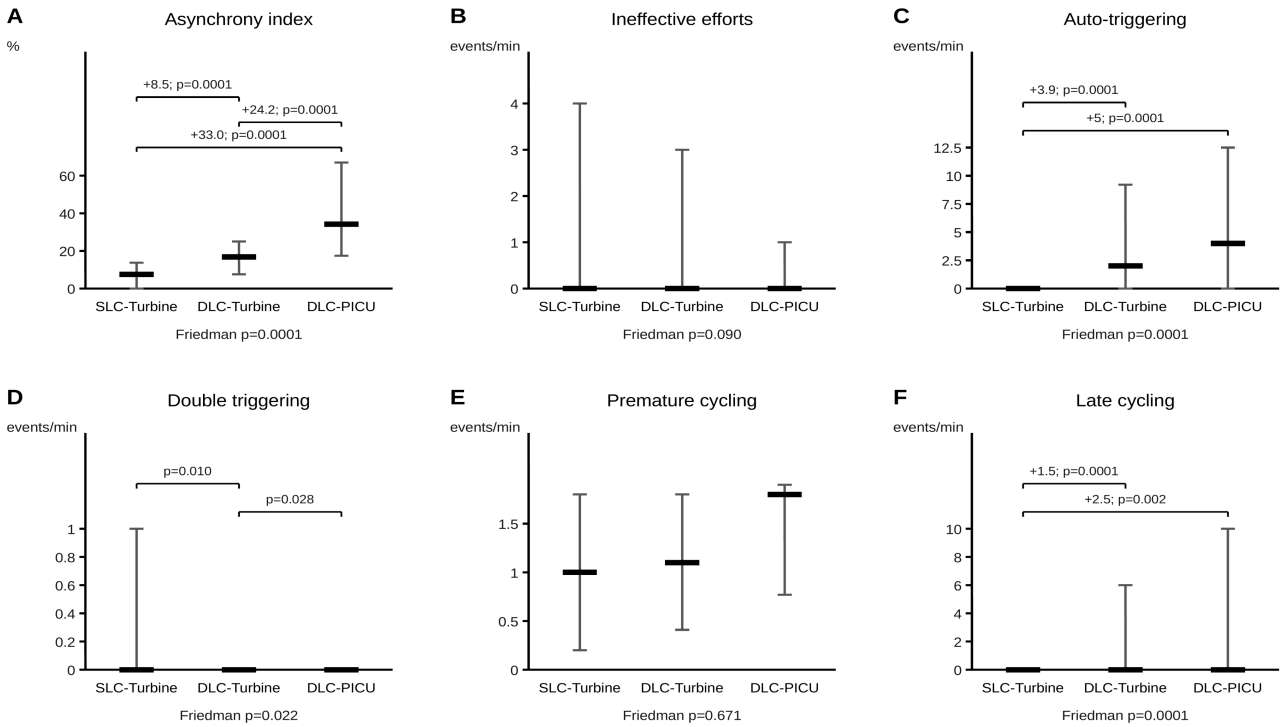


Figure 3

Patient–ventilator asynchronies across the three ventilator configurations.
Asynchrony Index (A) and asynchrony subtypes: ineffective efforts (B), auto-triggering (C), double triggering (D), premature cycling (E), and late cycling (F) during noninvasive ventilation with SLC-Turbine, DLC-Turbine, and DLC-PICU. All 12 infants are included; no recordings were excluded. Horizontal bars indicate the median and vertical lines the interquartile range. The p value below each panel refers to the overall Friedman test. Brackets show Hodges-Lehmann paired differences (first-named minus second-named condition) with the corresponding Wilcoxon signed-rank p value; only significant comparisons are displayed. For double triggering, the Hodges-Lehmann difference was 0 and only the p value is reported. No adjustment for multiple comparisons was applied. The primary comparison was DLC-PICU versus SLC-Turbine, the secondary comparison DLC-PICU versus DLC-Turbine, and the comparison between the two turbine

configurations was prespecified as exploratory. Abbreviations. DLC-PICU, pediatric intensive care unit ventilator with dual-limb circuit; DLC-Turbine, turbine-driven ventilator with dual-limb circuit and active expiratory valve; SLC-Turbine, turbine-driven ventilator with single-limb circuit and intentional leak.

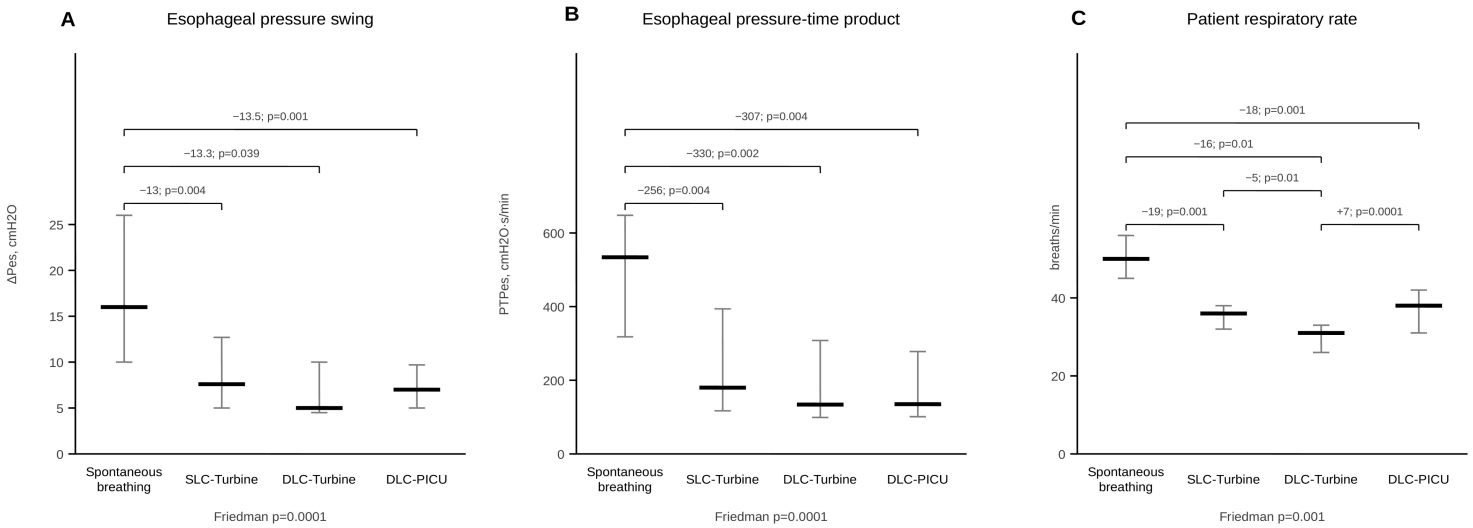


Figure 4

Respiratory effort and breathing pattern.

Esophageal pressure swing (A, ΔPes), esophageal pressure-time product (B, PTPes), and patient respiratory rate (C) during unassisted spontaneous breathing (SB) and noninvasive ventilation with SLC-Turbine, DLC-Turbine, and DLC-PICU. All 12 infants are included. Graphical conventions are as in Figure 3. Abbreviations. DLC-PICU, pediatric intensive care unit ventilator with dual-limb circuit; DLC-Turbine, turbine-driven ventilator with dual-limb circuit and active expiratory valve; ΔPes, esophageal pressure swing; PTPes, esophageal pressure–time product; SB, spontaneous breathing; SLC-Turbine, turbine-driven ventilator with single-limb circuit and intentional leak.

Supplementary Files

This is a list of supplementary files associated with this preprint. Click to download.

- AdditionalFile1MeasurementsandDefinitions.docx